NIPPON STEEL TECHNICAL REPORT No. 83 JANUARY 2001

UDC 669 . 782 : 620 . 19 ; 621 . 382

Nitrogen Doping Grown-in Defects Engineering in Silicon Crystals and Argon-annealed Wafer

Atsushi IKARI[*1] Akiyoshi TACHIKAWA[*1]
Hiroyuki DEAI[*1] Kazunori ISHISAKA[*1]
Hideki YOKOTA[*1] Jun TAKAHASHI[*1]
Toshiharu INOUE[*1] Katsuhiko NAKAI[*1]
Hideo KATO[*1] Toshiro FUTAGI[*1]
Yasumitsu OHTA[*1] Wataru OHASHI[*1]

Abstract

Over the last 30-years in the history of increasing shrinkage of the design rule and the high integration of integrated circuits, what was essential in the development and production of silicon crystals was the technology to control the characteristics of grown-in defects of Czochralski silicon crystals, especially octahedral voids and oxygen precipitates. This paper describes a defect engineering technology employing nitrogen doping capable of controlling both the voids and the oxygen precipitates. Nitrogen doping renders the voids to assume a tabular triclinic shape and to shrink in size and, at the same time, makes minute oxygen precipitates form in the crystals in high concentration. When heat-treated in an argon atmosphere, the crystals thus obtained will make ideal wafers having a defect-free surface layer showing excellent electric properties and a bulk with highly concentrated defects showing a high gettering capacity of impurities. This method produces excellent wafers at a cost lower than epitaxial wafers having equally good defect-free surfaces. Therefore, it is expected to offer wide applicability to the fabrication of a variety of devices for which low cost is needed.

1. Introduction

In the past 30 years, "defect engineering" in silicon wafers has been a keyword for the forefront of technology development in response to ceaselessly shrinking design rules and increasing integration density of devices, and has built the material science base of silicon wafers. "Microdefect engineering" or "oxygen precipitate engineering"[1] was developed in the 1980s, and "point defect engineering" or "void[2] defect engineering" became an unavoidable focus of interest in the 1990s.

The properties of Czochralski (CZ) silicon wafers for today's latest devices require high-reliability defect engineering of practically void-free wafer surfaces and surface layers to ensure gate oxide integrity (GOI) and pn junction leakage characteristics, and oxygen precipitate engineering as required for heavy-metal gettering with better stability and controllability in response to decrease process temperature. To meet these requirements, CZ crystal growth thermal history

*1 Technical Development Bureau

control, hydrogen annealing, and epitaxial layer deposition have been tackled to date as defect engineering means.

Nippon Steel Corporation (NSC) proposed nitrogen doping as a new defect engineering technology[3,4]. Nitrogen doping allows point defects and micro-defects, or voids and oxygen precipitates, to be simultaneously controlled in a desirable direction. Making use of this characteristic, the application of nitrogen doping to high-quality argon-annealed wafers and epitaxial wafers has been proposed. This report discusses the control of grown-in defects by nitrogen doping and the properties of argon-annealed wafers, and describes the effect of nitrogen doping on the defect formation mechanism.

2. Grown-in Defects in Nitrogen-doped Crystals

Nitrogen doping is reported to have the effects of reducing interstitial-type A defects and vacancy-type D defects in float zoning (FZ) silicon crystals[5,6], reducing the size and number of crystal-originated pits (COPs) in oxygen-doped OFZ crystals[7], and reducing the number of flow pattern defects (FPDs) in CZ silicon crystals[8]. Nitrogen doping is known to enhance oxygen precipitation to a considerable degree[9], therefore, denuded zone (DZ) formation by annealing was considered to be difficult[10].

2.1 Crystal and defect evaluation methods

To investigate how nitrogen doping would change grown-in defects, 6-inch and 8-inch P-type CZ silicon (100) single crystals were grown. The resistivity was 8 to 12 Ω·cm, and the oxygen concentration was 6 to 10×10^{17} atoms/cm^3 (JEIDA). The nitrogen concentration was measured by secondary ion mass spectroscopy (SIMS), and crystals with an average nitrogen concentration of 0.5 to 3×10^{15} atoms/cm^3 were used.

The density and size distribution of grown-in defects were investigated by using a 90° infrared light scattering tomograph (MO-4, Mitsui Mining & Smelting) and an optical precipitate profiler (OPP) (Bio-Rad) as methods for evaluating the grown-in defects. The morphology, microstructure, and composition of the grown-in defects were examined by transmission electron microscopy (TEM). The TEM observation of defects with a low density of 10^7/cm^3 or less involved investigating the position of defects near the wafer surface layer with a Brewster-angle LSTD scanner (MO-5, Mitsui Mining & Smelting), marking the defect positions with a laser, cutting the defect positions with a focused ion beam (FIB), and preparing TEM samples.

2.2 Nitrogen concentration dependence of grown-in defects

Fig. 1 shows the grown-in defects in as-grown crystals of different nitrogen concentrations as measured with the MO-4. The non-nitrogen-doped silicon has about 5×10^6/cm^3 of grown-in defects, which are considered to be octahedral voids according to past reports[11,12]. In the crystal with a nitrogen concentration of 3×10^{15} atoms/cm^3, grown-in defects are generated to a density of about 10^9/cm^3. The defect image contrast (the scatter intensity being proportional to the sixth power of the size) is smaller than in the non-nitrogen-doped crystal. In the crystal with a nitrogen concentration of 5×10^{14} atoms/cm^3, there are defects of contrast similar to that of defects present in the non-nitrogen-doped crystal, but there also are lower-contrast defects. From these results, it was found that there exist two types of grown-in defects in nitrogen-doped CZ silicon crystals and that the type of grown-in defect changes with the nitrogen concentration. The TEM results of the respective types of defects are discussed in the sections that follow.

2.3 Grown-in defects in crystals: Oxygen precipitates

Fig. 2 shows the TEM image of a grown-in defect observed in an as-grown crystal with a nitrogen concentration of 3×10^{15} atoms/cm^3. The grown-in defect density observed with the MO-4 was 10^9/cm^3 and was such that grown-in defects could be easily detected using plain-view TEM samples prepared by the conventional method. The defects are about 50 nm in size and have strong stain contrast. The grown-in defects observed in the nitrogen-doped crystal were analyzed by energy-dispersive X-ray spectroscopy (EDS). When the point a at which a defect is present is compared with the point b at which the silicon matrix is analyzed, the point a has more nitrogen and oxygen detected than the point b. This shows that the defect is a nitrogen-containing oxygen precipitate. The nitrogen doping rate being equal, the grown-in defects increase in size with decreasing V/G ratio (**Fig. 3**).

The defect lies on the {100} plane, is shaped like a platelet, and is similar in morphology to oxygen precipitates formed when the non-nitrogen-doped crystal is annealed at or under 1,000°C. The annealing-induced platelet oxygen precipitates exhibit a dendritic structure inside a square platelet structure when they increase in size. The defects observed in the nitrogen-doped crystal reveal no such structure, and are greatly changed in shape from the square.

2.4 Grown-in defects in crystals: Triclinic void defects

Fig. 4 shows the TEM image of grown-in defect observed in an as-grown crystal with a nitrogen concentration of 6.5×10^{14} atoms/cm^3. The defect density was about 10^7/cm^3, and the TEM sample was prepared by marking with the MO-5. Fig. 4 differs from Fig. 3 in that no strain field is present around the defect. When the defect

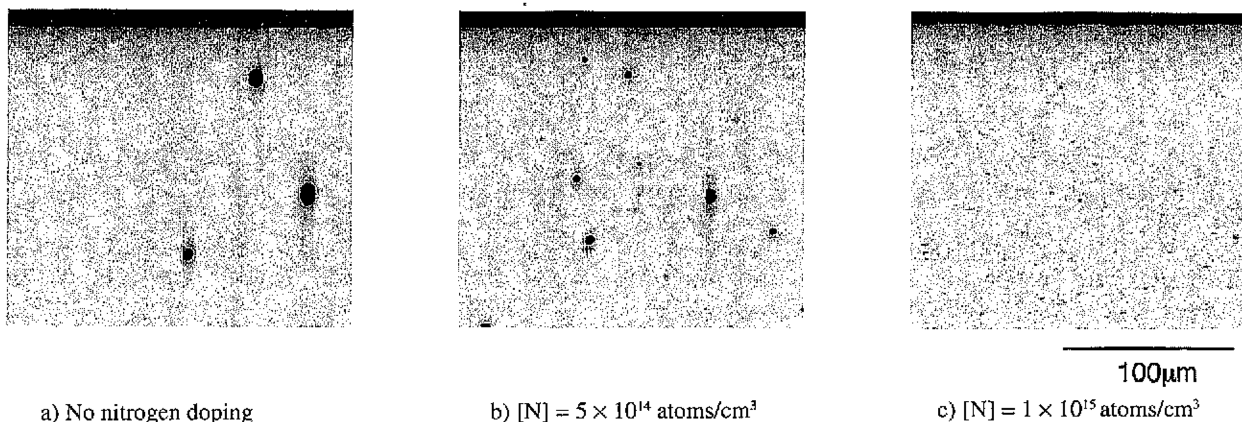

a) No nitrogen doping b) [N] = 5×10^{14} atoms/cm^3 c) [N] = 1×10^{15} atoms/cm^3

Fig. 1 Observation of grown-in defects with infrared tomograph (MO-4)

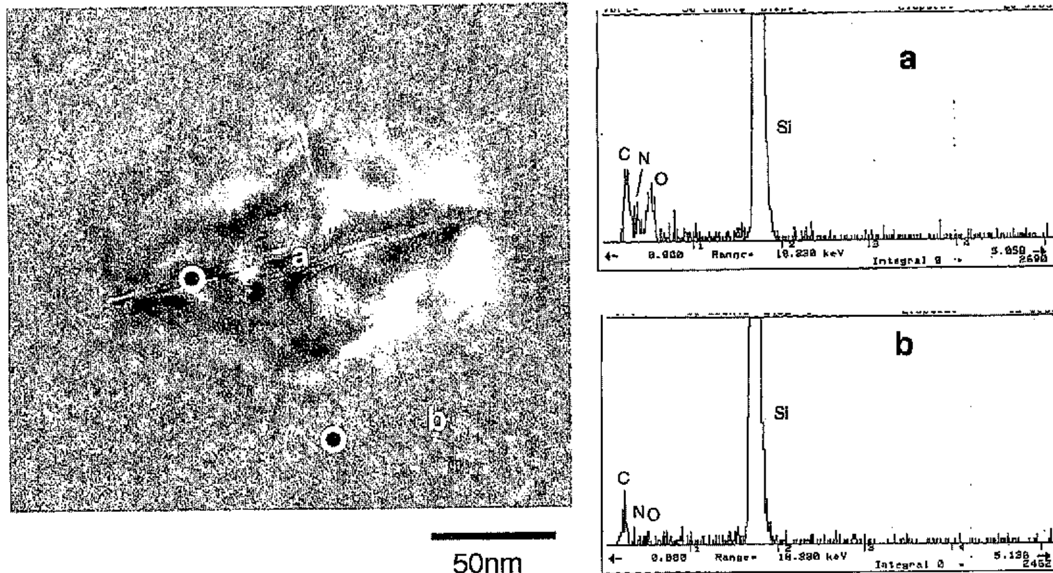

Fig. 2 EDS analysis of grown-in defects in crystal with [N] = 3×10^{15} atoms/cm^3

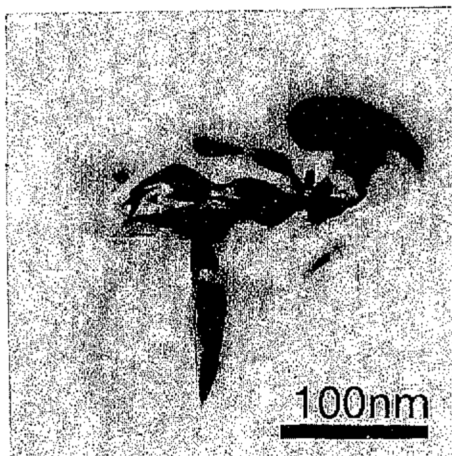

Fig. 3 Grown-in defect in crystal with [N] = 3×10^{15} atoms/cm^3 and grown at low V/G ratio

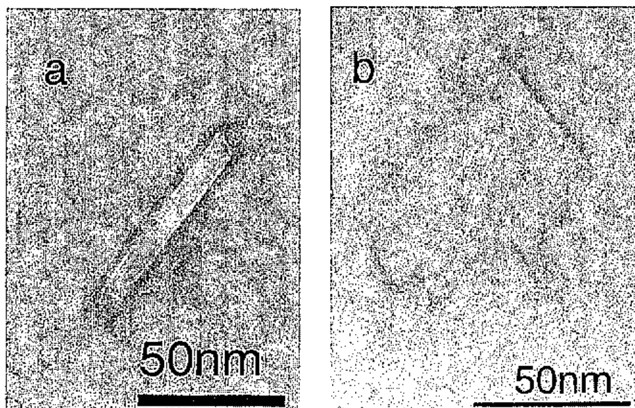

Fig. 4 a) Grown-in defect in crystal with [N] = 6.5×10^{14} atoms/cm^3 and grown at high V/G ratio (observed in <100> direction); b) Same grown-in defect observed by tilting crystal 15° each in horizontal and vertical directions

position was analyzed by EDS, the presence of oxygen was unclear. These findings suggest that the defect is a void[8]. The defect was about 70 nm × 10 nm in size and rodlike in morphology when observed in the <110> direction, but was found to expand in a platelet form as shown in Fig. 4 (b) when the sample was observed by tilting it 15° each from the <110> direction to the <$1\bar{1}0$> direction and to the <001> direction.

The side angles of the defect were measured, and its spatial structure was observed by considering the tilt angle of the sample. As shown in **Fig. 5**, the platelet void was found to be a triclinic enclosed by the {111} planes. When the average volume of a void was calculated from these observation results and was multiplied by the defect density measured with the OPP, the total void volume (the total volume of voids contained in 1 cm^3) was (2.2×10^4 nm^3) × (2×10^7/cm^3) = 4.4×10^{11} nm^3/cm^3 and was of approximately the same order as the total void volume of the non-nitrogen-doped crystal (7.2×10^{11} nm^3/cm^3).

The void defect changes its shape when the nitrogen concentration is lower at 2.1×10^{13} atoms/cm^3. It shape is no longer a triclinic but is close to an octahedron as seen in the non-nitrogen-doped crystal (**Fig. 6**). The defect does not accompany a strain field either and is considered to be a void. The planes enclosing the void are not flat

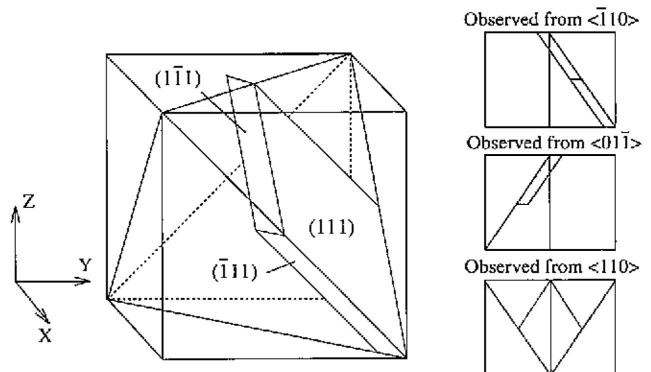

Fig. 5 Triclinic parallelepiped

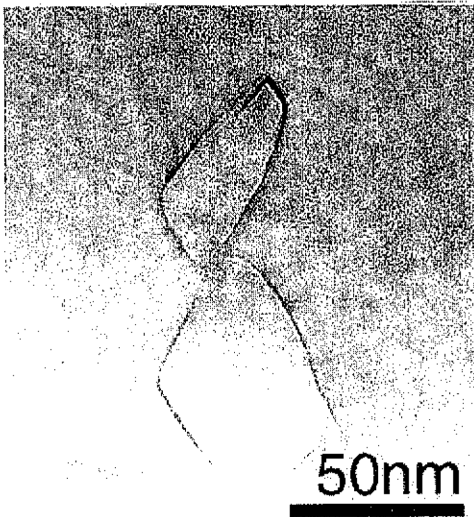

Fig. 6 Grown-in defect in crystal with [N] = 2.1×10^{13} atoms/cm^3 and grown at high V/G ratio

{111} planes, but appear round on the whole. When the total void volume of the crystal is obtained, it is (8.7×10^4 nm^3) × (9.2×10^6/cm^3) = 8.0×10^{11} nm^3/cm^3. It was larger than the total void volume of the aforementioned nitrogen-doped crystal and equivalent to the total void volume of the non-nitrogen-doped crystal.

2.5 Dependence of grown-in defects on nitrogen concentration and growth conditions

To investigate the nitrogen concentration dependence of the density of oxygen precipitates existing in the as-grown condition, silicon single crystals were annealed in a nitrogen ambient at 1,000°C for 16 h and was measured with the MO-4. The results are shown in **Fig. 7**. Oxygen does not precipitate when the crystal is not doped with nitrogen, but the oxygen precipitate density increases with increasing nitrogen doping rate when the crystal is doped with nitrogen. This oxygen precipitate density does not change when the crystal is two-step heat treated at 800°C for 4 h and at 1,000°C for 16 h, for example. The oxygen precipitation of the nitrogen-doped crystal is low in dependence on the initial oxygen concentration, and the nitrogen-doped crystal exhibits constant oxygen precipitation in a wide initial oxygen concentration region.

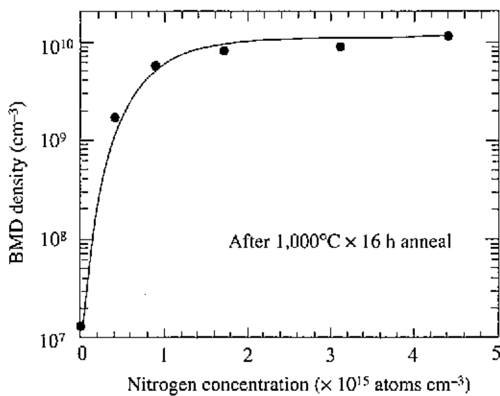

Fig. 7 Oxygen precipitate density of nitrogen-doped crystal after annealed at 1,000°C for 16 h

The nitrogen concentration dependence of the density and size of triclinic voids was measured with the OPP. The results are shown in **Figs. 8** and **9**, respectively. The voids decrease in both volume density and size with increasing nitrogen concentration. The method of repeatedly cleaning the crystal in SC-1 solution and measuring the voids in the crystal with a surface particle counter produces the same change in density as obtained with the OPP.

The distribution of defects in the radial direction of nitrogen-doped crystals was evaluated after OSF oxidation, using X-ray topographs. A pulling condition of a high V/G ratio form R-OSF in the periphery of the crystal when the crystal is not nitrogen doped. When the crystal is nitrogen doped, the OSF region increases in width, and the void region decreases. As the V/G ratio decreases, the OSF region shrinks toward the center of the crystal, and a dislocation region eventually appears in the periphery of the crystal. It should be noted that the boundary between the dislocation region and the OSF region is clear, but that the boundary between the void region and the OSF region is unclear. A map of grown-in defects as arranged by the nitrogen concentration and the V/G ratio is shown in **Fig. 10**.

The TEM observation results in this experimental work may be arranged by the grown-in defect map as shown in **Fig. 11**. Voids are generated in the V region. When the V/G ratio is kept constant and the nitrogen concentration is increased, the voids change in morphology from octahedrons to triclinic. Oxygen precipitates are observed in the OSF region and increase in size with increasing V/G

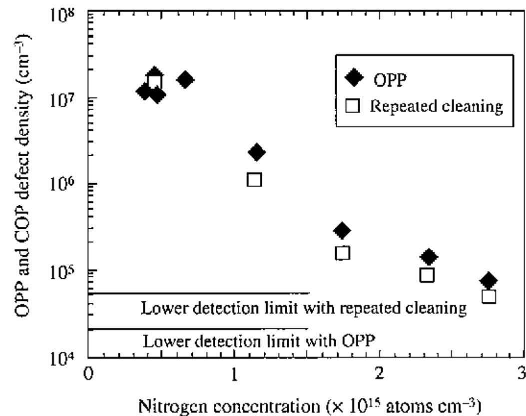

Fig. 8 Reduction in void density by nitrogen doping

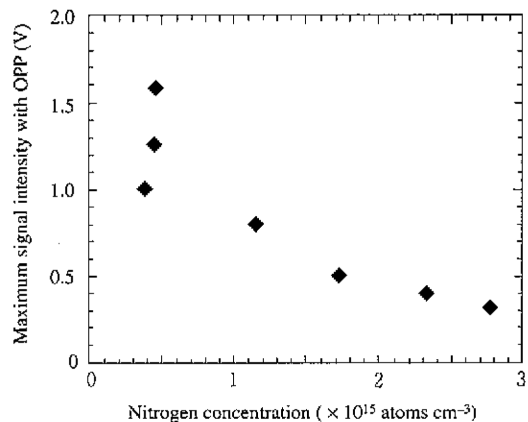

Fig. 9 Reduction in void size by nitrogen doping

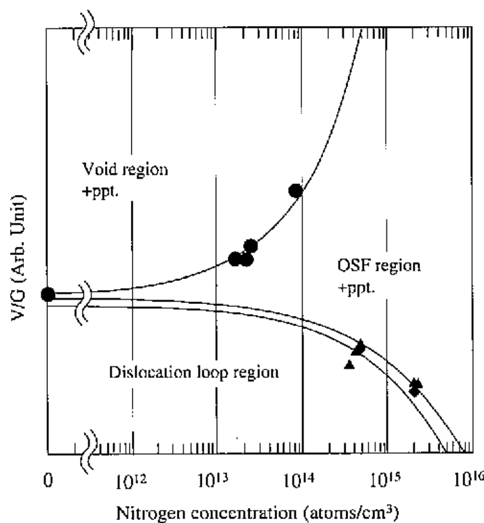

Fig. 10 Generation behavior of grown-in defects in nitrogen-doped crystals

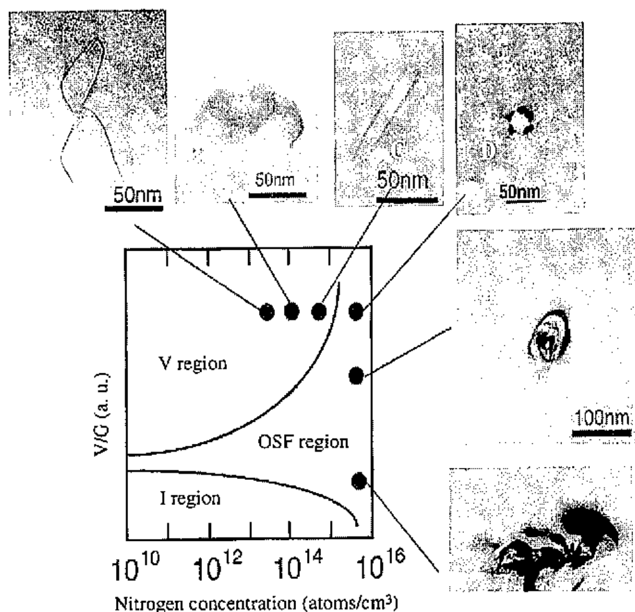

Fig. 11 Summary of TEM observation results

ratio. It may be reasonable to think that since the experiment held G constant and changed V, the crystal cooling time increased to increase the time for the growth of the oxygen precipitates.

In the non-nitrogen-doped crystal, as-grown oxygen precipitates are not confirmed in any regions other than the region where OSFs are formed in a ring[13]. In the nitrogen-doped crystal, oxygen precipitates are already formed in the as-grown condition. These oxygen precipitates are considered to nucleate the oxygen precipitates to be generated when the above-mentioned OSF region is annealed. Oxygen precipitates could not be confirmed in the V region. Annealing produces oxygen precipitates in the V region like in the OSF region. This means that some oxygen precipitates are formed in the V region in the as-grown condition. Such a situation could not be observed by TEM, probably because the oxygen precipitates in the V region are much smaller than those in the OSF region and the strain field in the V region is also small.

2.6 Clarification of mechanism of grown-in defect formation in nitrogen-doped crystal by growth holding experiment

When the pulling of a crystal is stopped during its growth and the crystal is examined, what defect is formed at what temperature during crystal growth can be estimated just as if snap shots of the crystal are looked at. This method was used to estimate the formation and growth temperature regions of voids in non-nitrogen-doped crystals. The void formation and growth temperature regions in nitrogen-doped crystals as investigated by the method are shown in **Figs. 12** and **13**. It is evident that the void formation and growth temperatures decrease with increasing nitrogen doping rate. A precipitation retarded region (or region where the amount of precipitation is small when the crystal is annealed) exists at lower temperatures. It was found that the temperature at the low-temperature boundary of the precipitation retarded region or the precipitation restart temperature change little with nitrogen doping but slightly increases.

The reduction in the void size and the defect formation temperature by nitrogen doping may be explained by the reduction in the effective supersaturated concentration of vacancies by nitrogen doping. When solid reactions[14] are considered, void nucleation can be simply expressed by a product of the atomic frequency, index of activation energy for the movement of vacancies, total number of vacancies, and index of free energy for critical nucleation. Three scenarios can be then considered: change in activation energy for the

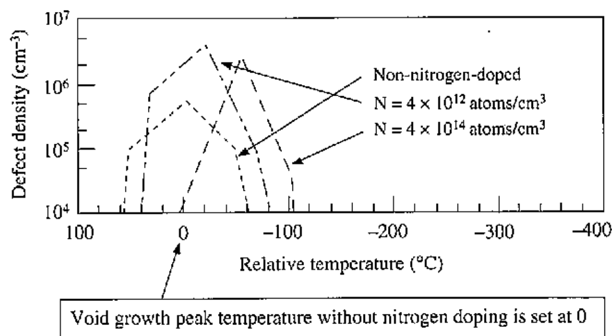

Fig. 12 Reduction in void growth temperature by nitrogen doping

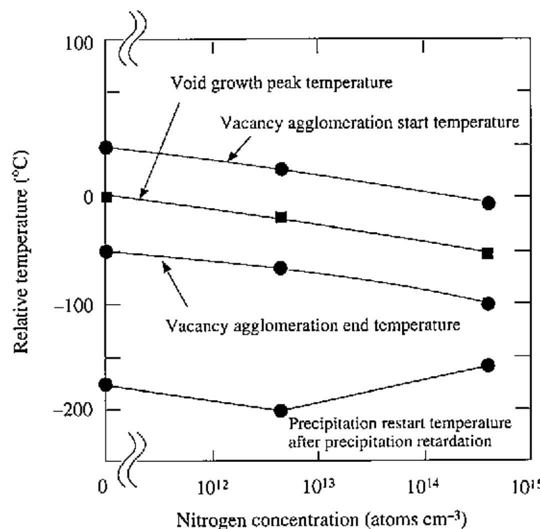

Fig. 13 Void formation and growth temperatures of nitrogen-doped crystals as investigated using pulling-hold crystals

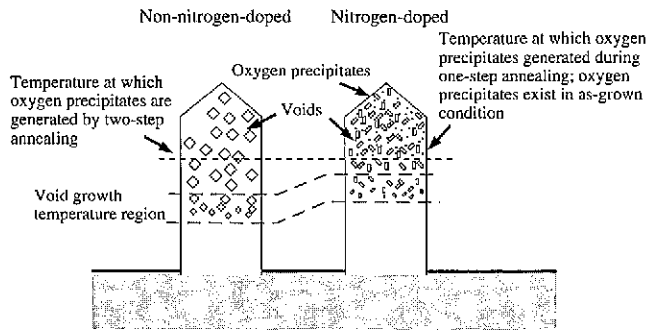

Fig. 14 Defect formation mechanism

migration of vacancies by nitrogen, reduction in the total number of vacancies by nitrogen, and reduction in free energy for critical nucleation by nitrogen. In the first two scenarios, the void formation temperature shifts to the low end of the temperature range. The cumulative void volume in the nitrogen-doped crystals does not appreciably change as already noted. This suggests that nitrogen has only a small effect on the total number of vacancies.

Nitrogen doping shifts the void formation temperature to the low end of the temperature range[15]. It is now considered reasonable to think that nitrogen reduces the migration of vacancies (bulk diffusion or void interface). The vacancies and nitrogen atoms in crystals both number about 10^{14} to 10^{15}/cm^3. The results of the first-principle calculation show that the nitrogen atom pairs combine with the vacancy pairs[16].

The formation mechanism of grown-in defects in nitrogen doping is thought to be as follows. The nitrogen atom pairs interact with the vacancy pairs and reduce the mobility of vacancies in the crystal. The reduced mobility of vacancies lowers the effective supersaturated concentration of vacancies and shifts the void nucleation temperature to the low end of the temperature range. As a result, vacancies that have not transformed to voids and accompany nitrogen atom pairs, or what may be called frozen vacancies, eventually act as nucleation sites for high-density oxygen precipitation at or under 1,000°C (this precipitation temperature is changed little or slightly raised by nitrogen doping). When the as-grown oxygen precipitates are large in size, the region becomes the OSF region (**Fig. 14**).

3. Growth and Annihilation of Defects in Nitrogen-Doped Crystals by Argon Anneal

Annealing a conventional wafer in a hydrogen ambient[17] is known as "high-wafer". Hydrogen annealing had the problem of a small surface denuded zone thickness of only about 1 μm. In its initial development phase, hydrogen annealing was recognized to be able to reduce defects in any crystals. It was investigated whether or not the denuded zone thickness could be increased further by changing staring crystals to be annealed, and it was studied in depth what would be ideal crystals for annealing. It was found that nitrogen doping as discussed above can control defects generated during crystal growth and helps to produce annealed wafers with a deeper denuded zone and with a higher density of oxygen precipitates in the bulk as gettering sites[3, 18-22].

One claimed advantage of using hydrogen is that the oxygen concentration in the surface layer can be lowered nearly to zero. It is reported that a similar effect can be achieved by annealing in an inert gas like argon[23]. Annealing was thus performed in an atmosphere of easy-to-use argon.

3.1 Growth of grown-in oxygen precipitates by annealing

It was found that oxygen precipitates are generated in nitrogen-doped crystals to such a high density as shown in Fig. 1 (c). When the nitrogen-doped crystal is annealed, oxygen precipitation becomes simple in behavior because it only involves the growth of the oxygen precipitates already formed during crystal growth. The oxygen precipitation behavior in the non-nitrogen-doped crystal is generally complicated. **Fig. 15** shows the change in the density of oxygen precipitates generated in the non-nitrogen-doped crystals when the non-nitrogen-doped crystals are isochronally annealed. From Fig. 15, it can be seen that the precipitate density greatly changes with the annealing temperature. In actual precipitation, there occurs a incubation time until the start of precipitation. The length of this incubation time changes with the annealing temperature and adds to the complexity of the precipitation behavior.

Non-nitrogen-doped crystals were similarly isochronally annealed, and the density of oxygen precipitates was measured with the MO-4. The results are shown in **Fig. 16**. The precipitate density is almost constant, irrespective of the annealing temperature and time. The precipitate density of the annealed crystals is higher than the as-grown precipitate density, or a low precipitate density is obtained

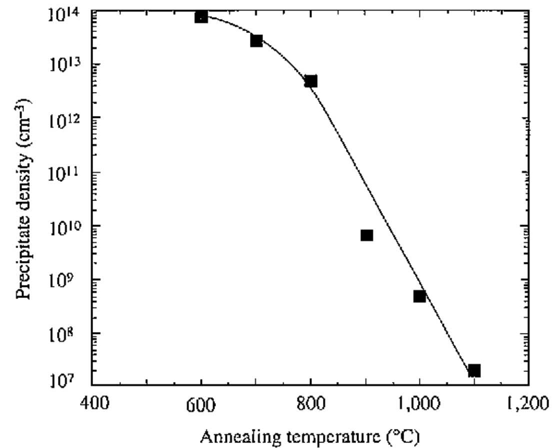

Fig. 15 Precipitate density in non-nitrogen-doped crystal during 128-h isochronal annealing

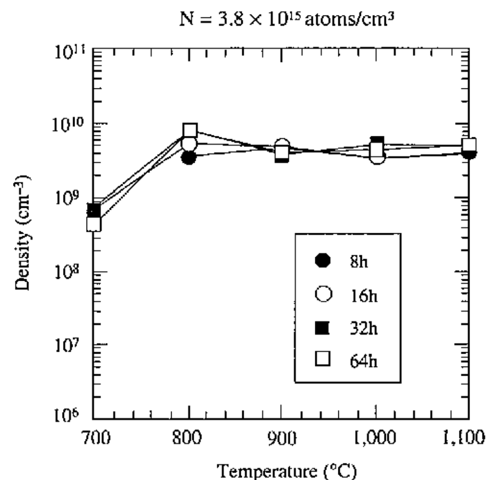

Fig. 16 Change in precipitate density in crystals with [N] = 3.8×10^{15} atoms/cm^3 during isochronal annealing

with a low-temperature annealing, because the sensitivity of the MO-4 is not high enough to measure small precipitates in the as-grown condition or annealed at a low temperature. This result shows that the oxygen precipitation behavior of the nitrogen-doped crystals can be represented by a simple model that assumes that the density of oxygen precipitates already present in the as-grown condition is constant.

This simple oxygen precipitation characteristic can be utilized to produce ideal wafers having an excellent defect-denuded zone in the surface and high-density oxygen precipitate gettering sites in the bulk. This characteristic of producing a high density of oxygen precipitates can be used to provide epitaxial wafer substrates with an excellent gettering capability. The application of nitrogen-doped crystals to epitaxial wafers is described in another paper in this special issue of the NSTR.

3.2 Annihilation of grown-in voids and control of surface integrity by argon annealing

High-temperature argon annealing was conducted to obtain high-quality wafer properties by making use of the characteristics of voids and as-grown oxygen precipitates whose formation behavior are deeply influenced by nitrogen doping. Wafers were annealed in a high-purity argon ambient at 1,100°C, 1,150°C and 1,200°C, polished by 1, 3 and 5 μm, and cleaned 10 times in a SC-1 solution. The COPs in the surface layer of each wafer were then measured with the surface particle counter. The volume density and count of COPs in each wafer are shown in **Fig. 17**. The nitrogen-doped wafer exhibits a stable and good COP annihilation behavior at all levels. For example, the annealing temperature dependence is low, and good COP annihilation occurs at 1,100°C.

The COP annihilation of the conventional, non-nitrogen-doped wafer strongly depends on the annealing temperature and depth from the surface. The COPs in the nitrogen-doped wafers can be removed to a level below the detection limit of the surface particle counter if the annealing conditions are optimized. The good surface defect free zone of the argon-annealed, nitrogen-doped wafers can be readily seen from the results of measurement with the LSTD scanner MO-6 that can scan the entire wafer surface at a time (**Fig. 18**).

Wafers argon-annealed at the specific temperatures were annealed by two-step precipitation annealing and CMOS heat simulation, and were measured for the density of bulk microdefects (BMDs). The BMD density of the annealed, nitrogen-doped wafers was higher by an order of magnitude than that of the non-nitrogen-doped wafers, and was not less than $5 \times 10^9/cm^3$ after any annealing. The non-nitrogen-doped wafers tended to slightly decrease in the BMD density with increasing annealing temperature. The oxygen precipitate-denuded zone in the nitrogen-doped wafers was stable and unchanged after each annealing, despite the high oxygen precipitate density.

To investigate the gate oxide integrity (GOI) of the wafers, their time-zero dielectric breakdown (TZDB) characteristics were measured. The gate area was 20 mm^2, and the gate oxide thickness was 25 nm. The proportion of wafers that exhibited a dielectric breakdown voltage of 8 MV/cm at a threshold current of 1 $\mu A/cm^2$ was measured as a low-C mode, and the proportion of wafers that exhibited a dielectric breakdown voltage at a threshold current of 100 mA/cm^2 was measured as a high-C mode. As shown in **Fig. 19**, the near-surface dielectric performance of the non-nitrogen-doped crystals is greatly improved by argon annealing. When the dielectric performance after 1-μm mirror polishing is examined, it is evident that the nitrogen-doped crystals have wafer surface defects annihilated to a greater depth. For comparison under more severe conditions, TDDB measurements were made with a gate area of 50 mm^2 and gate oxide thickness of 24.8 nm. The results are shown in **Fig. 20**. The conventional wafers instantaneously failed, whereas the argon-annealed, nitrogen-doped wafers exhibit excellent TDBD characteristics.

The nitrogen-doped wafers have a high density of oxygen precipitates formed in the as-grown condition and have voids reduced in size or annihilated. When such a wafer is annealed in a nonoxidizing, high-purity argon ambient, the defects are efficiently annihi-

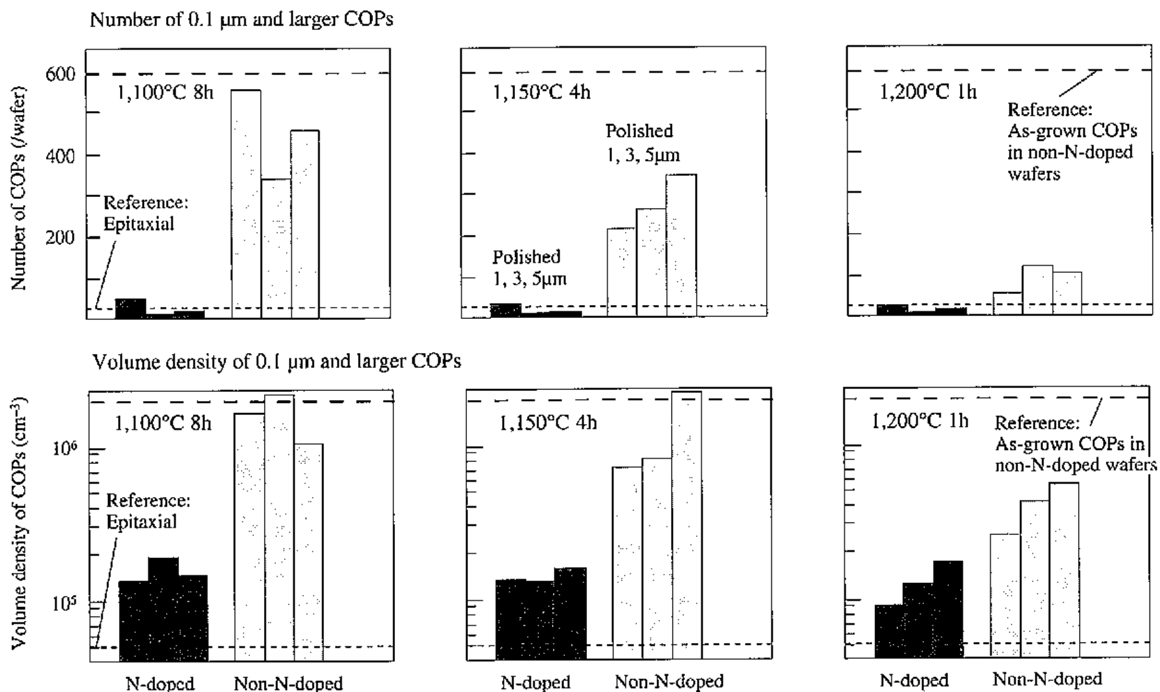

Fig. 17 Surface COP density in wafers made from nitrogen-doped crystals and argon annealed at 1,150°C for 4 h

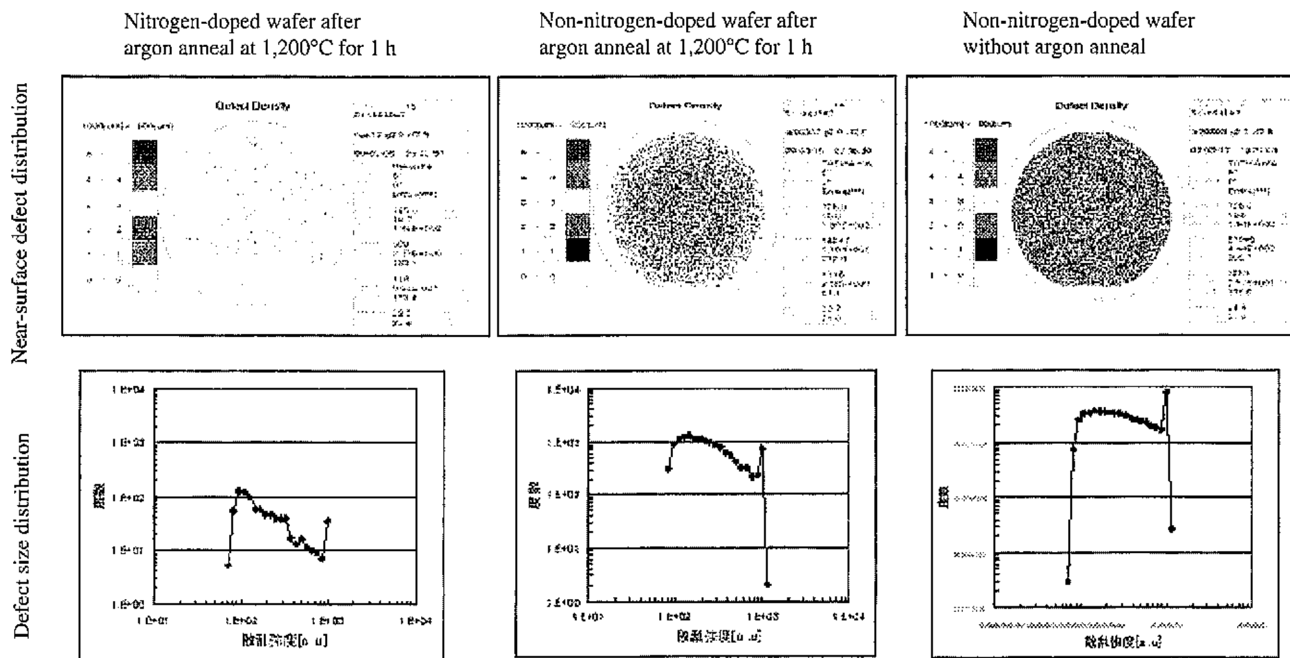

Fig. 18 Surface defect comparison of wafers with MO-6

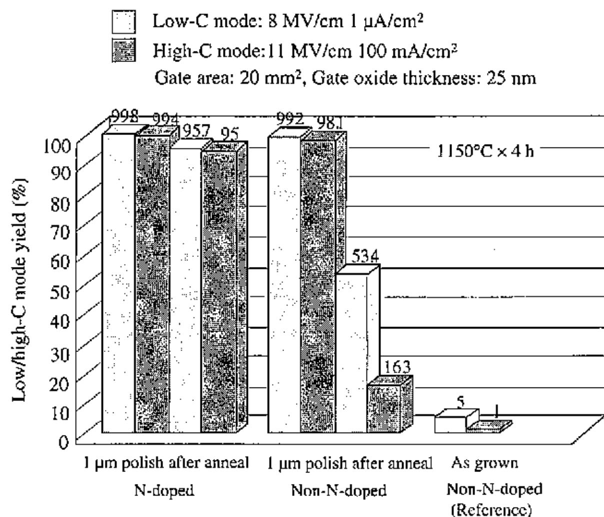

Fig. 19 TZDB test results of wafers made from nitrogen-doped crystals and argon annealed at 1,150°C for 4 h

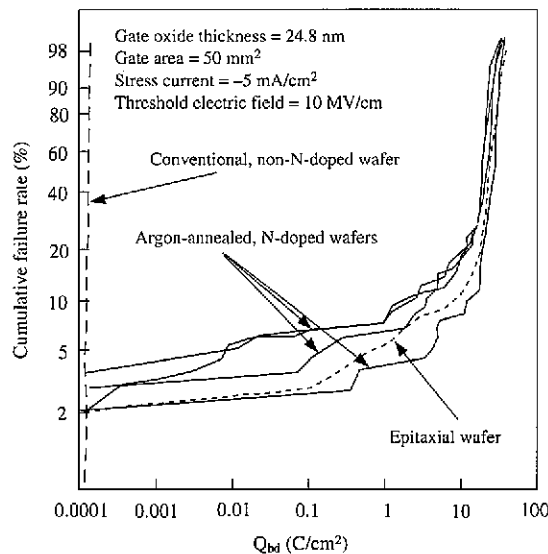

Fig. 20 TDDB test results of wafers made from nitrogen-doped crystals and argon annealed at 1,200°C for 1 h

lated in the oxygen-unsaturated surface zone and grow in the oxygen-supersaturated bulk. As a result, two contracting objectives, or defect free surface for excellent electrical properties and formation of high-density bulk defects for heavy-metal gettering, can be achieved at the same time.

4. Conclusions

The technology developed for engineering defects by nitrogen doping can limit the formation of voids, a traditional problem, change the morphology of voids into triclinic platelet form, and reduce the size of voids by controlling the mobility of point defects during crystal growth. At the same time, high-density oxygen precipitates can be formed in the crystal. When the crystal is argon annealed, it can be used to produce an ideal wafer that meets the contradicting requirements of a surface defect-denuded zone with excellent electrical properties and a bulk microdefect region with a high density and high impurity gettering capability. The defect engineering technology has been already applied to provide epitaxial wafers with gettering capability and is expected to find use in various other applications. The nitrogen doping-based defect engineering technology is expected to mark a turning point to a new impurity age in the semiconductor manufacturing field where lower cost and higher integration must be accomplished at the same time.

References

1) Tan, T. Y.: Appl. Phys. Lett. 30, 175 (1977)
2) Ryuta, J. et al.: J. J. Appl. Phys. 29, L1947 (1990)
3) Ohashi, W.: The 46th Annual Meeting Extended Abstracts, 29a-ZB-1, The Japan Society of Applied Physics, 1999
4) Kobayashi, T. et al.: The 46th Annual Meeting Extended Abstracts, 29a-ZB-8, The Japan Society of Applied Physics, 1999
5) Abe, T. et al.: VLSI Sci. and Tech. ECS, Pennington, 1985, p.543
6) Ammon, W. V. et al.: ECS Proceedings. 98-1, Abst. No.512, 1998
7) Graf, D. et al.: ECS Proceedings. 96-13, Abst. No.117, 1996
8) Yamagishi, H. et al.: Japan Society for the Promotion of Science, The 145 Committee, Symposium on Advance Science and Technology of Silicon Mater. Hawaii, 1991, p.83
9) Chiou, H. D. et al.: ECS Spring Mtg. Extended Abst. No.36, 1984
10) Shimura, F., Hockett, R. S.: Appl. Phys. Lett. 48, 224 (1986)
11) Itsumi, M. et al.: J. Appl. Phys. 78, 5984 (1995)
12) Mera, A. et al.: Applied Physics. 66, 728 (1997)
13) Nakai, K. et al.: The 46th Annual Meeting Extended Abstracts, 29p-ZB-8, The Japan Society of Applied Physics, 1999
14) Becker, R.: Proc. Phys. Soc. 52, 71 (1940)
15) Iida, M. et al.: The 60th Annual Meeting Extended Abstracts, 3a-ZY-1, The Japan Society of Applied Physics, 1999
16) Sawada, H. et al.: Proc. of the Kazusa Academia Park Forum on the Science on Technology of Silicon Materials '99. 1999, p.105
17) Matsushita, Y. et al.: Proc. of 18th Conf. on Solid State Devices & Mater. Tokyo, p.529
18) Nakai, K. et al.: J. Jpn. Assoc. Cryst. Growth. 26, 250 (1999)
19) Ikari, A. et al.: Solid State Phenomena, 69-70, 161 (1999)
20) Ohashi, W.: Proc. of the Kazusa Academia Park Forum on the Science on Technology of Silicon Materials '99. 1999, p.80
21) Ikari, A. et al.: The 46th Annual Meeting Extended Abstracts, 29a-ZB-2, The Japan Society of Applied Physics, 1999
22) Yokota, H. et al.: The 46th Annual Meeting Extended Abstracts, 29a-ZB-3, The Japan Society of Applied Physics, 1999
23) Yamada, N., Yamada-Kaneta, H.: Proc. of the Kazusa Academia Park Forum on the Science on Technology of Silicon Materials '97. p.468, 1997